

Optimizing infrared drying of black soldier fly larvae for sustainable cricket feed production

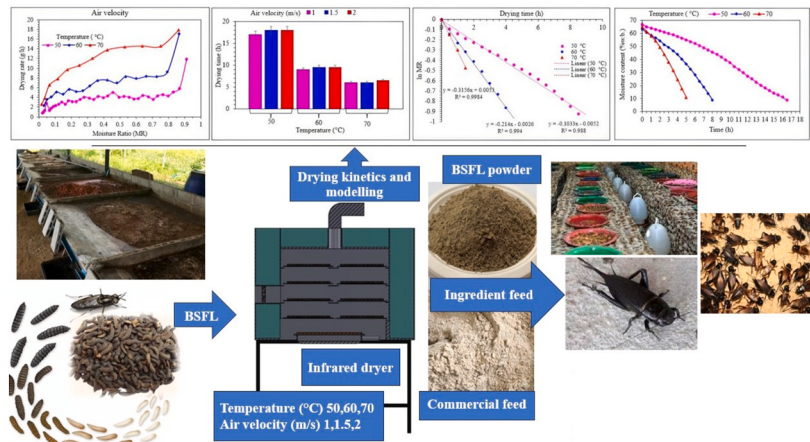
Nuntawat Butwong^a, Sarawut Saenkham^a, Adisak Pattiya^a, Anuwat Saenpong^b, Chinnapat Turakarn^b, Aphichon Mungchu^b, Shenghua Hu^c, Sopa Cansee^{a,*}

^a Faculty of Engineering, Mahasarakham University, Kantarawichai, Maha Sarakham, 44150, Thailand

^b Department of Mechanical and Mechatronics Engineering, Engineering and Industrial Technology, Kalasin University, 46000, Thailand

^c Electrical and Mechanical Engineering, Qingyuan Vocational High School, Lishui City, Zhejiang Province, 323800, China

GRAPHICAL ABSTRACT



ARTICLE INFO

Keywords:

Black soldier fly larvae
Infrared radiation
Drying kinetic
Modeling thin layer drying

ABSTRACT

As global demand for animal-derived protein surges, Black soldier fly larvae emerge as a promising sustainable feed source, particularly for cricket farming. This study investigated the infrared drying of whole larvae, exploring its potential as an efficient alternative to conventional drying methods for producing high-quality cricket feed. The effects of temperature (50 °C, 60 °C, 70 °C)

* Corresponding author.

E-mail address: sopa.c@msu.ac.th (S. Cansee).

and air velocity (1.0, 1.5, 2.0 m/s) on drying behavior, energy consumption, and moisture diffusivity were examined. Higher temperatures significantly reduced drying time, with 70 °C leading to the fastest drying in ~5 h. While air velocity had minimal impact on overall drying time, it influenced drying rates. The optimal specific energy consumption was 1.58 MJ/kg water evaporated at 60 °C. The Logarithmic and Midilli models best described the drying kinetics, with $R^2 > 0.99$. Effective moisture diffusivity ranged from 2.28×10^{-9} to $3.09 \times 10^{-8} \text{ m}^2/\text{h}$, increasing with temperature. Activation energy values spanned from 56.88 kJ/mol at 1.0 m/s to 115.41 kJ/mol at 2.0 m/s air velocity. This study demonstrated that infrared drying offered a balanced approach for larvae processing, providing faster drying times and moderate energy consumption compared to hot air and solar drying, making it a viable option for producing sustainable cricket feed.

1. Introduction

The global demand for animal-derived protein is surging, driven by a rising population and improving living standards, particularly in developing countries [1]. As resources become scarcer, the prices of animal feedstock have surged, accounting for 60–70 % of production costs in animal farming systems and leading to competition between food sources for humans and animals [2,3]. The rising use of ingredients like fishmeal, soybean meal, and grains in both human food and animal feed further exacerbates this issue [2]. Insects, such as the black soldier fly larvae (BSFL), offer a promising solution due to their high protein content, efficient feed conversion, and rapid growth rates [4,5], making them a potentially profitable alternative feedstuff for production animals [6–8].

The black soldier fly (*Hermetia illucens*), native to the Americas and prevalent across tropical and temperate regions [9], is increasingly recognized for its potential as a sustainable feed source [10]. The fly larvae stand out among other insect species, including the yellow mealworm (*Tenebrio molitor*), due to its polyphagous nature and the high enzymatic activity of its gut extracts, which include amylase, lipase and protease [11,12]. These enzymes allow the larvae to efficiently break down and recycle a wide range of organic waste [13–17] transforming bio-waste into a high-quality nutrient source for animal feed [18]. While yellow mealworms are also a viable source of protein and have been used in animal feed, they primarily thrive on a diet of cereals and grains, which limits their ability to process diverse organic waste materials. In contrast, these larvae can consume a broader range of organic substrates, including manure [19–21], food scraps and agricultural by-products [22–24], making them a more versatile and sustainable option for waste management and feed production [13]. Moreover, these larvae have a higher feed conversion efficiency compared to yellow mealworms, meaning they require less feed to produce the same amount of biomass [24]. This efficiency, combined with their rapid growth rate, makes these larvae a cost-effective choice for producing high-quality protein for livestock, including swine, poultry and fish. Additionally, the larvae are being studied as a crucial ingredient for pet food, further broadening their application as a sustainable feed source [25]. Thus, the larvae emerge as the optimal choice for inclusion in cricket feed, particularly in regions where sustainable and cost-effective feed alternatives are urgently needed. Their ability to use a wide range of organic matter and convert it into high-quality protein makes them a superior choice compared to yellow mealworms, especially for large-scale feed production [2].

Drying is a critical step in processing the larvae as it affects both the quality and economic viability of the product. Effective drying ensures a stable product with a longer shelf life, while inefficient methods may lead to nutrient loss, increased production costs and limited scalability [26]. Several larval drying methods have been studied, each presenting specific benefits and challenges. Hot air drying is one of the most commonly used methods due to its simplicity and feasibility for large-scale operations. It works by circulating hot air around the larvae to evaporate moisture [27]. Although effective, conventional hot air drying can be energy-intensive and may require extended drying times that contribute to nutrient loss, particularly of heat-sensitive components such as proteins and lipids [4]. To mitigate these effects, previous studies have recommended optimizing drying parameters, such as temperature and airflow rate [28]. Infrared (IR) drying presents an innovative alternative, using near-infrared (NIR) or far-infrared radiation (FIR) to transfer heat directly to the surface of the material being dried, thus reducing energy consumption by avoiding the need to heat ambient air [29]. FIR, in particular, is highly effective in food processing, due to its strong absorption by most food ingredients [29–32]. Additionally, IR drying offers several advantages, including lower drying costs, more uniform heating, and the ability to control the drying process more precisely [33]. While IR drying has been applied successfully to many food products [30,34], its potential for processing the fly larvae into a high-quality cricket feed ingredient remains underexplored.

The primary motivation for this study stemmed from the urgent need to develop sustainable and cost-effective feed alternatives for cricket farming, addressing the challenges of rising feed costs and resource scarcity. Despite the potential of the larvae as a feed ingredient, there is a significant knowledge gap in optimizing their processing, particularly in the crucial drying stage. This research was driven by the need to enhance the efficiency and quality of processing the larvae, thereby contributing to the broader goal of sustainable insect farming and protein production.

The contributions of this work are threefold. Firstly, it comprehensively analyzed infrared drying of whole larvae, offering insights into the effects of temperature and air velocity on drying kinetics and energy efficiency. This information is crucial for optimizing large-scale production of the larvae as a feed ingredient. Secondly, it evaluated infrared drying as a potentially superior method for larvae processing compared to conventional hot air drying, addressing industry needs for more efficient and cost-effective processing. Lastly, it established a foundation for future research into the use of infrared-dried larvae in cricket feed, potentially significantly enhancing the sustainability and economics of cricket farming.

This study addressed this gap by optimizing the infrared drying process for these larvae, by evaluating the effects of drying

parameters - temperature and air velocity - on drying characteristics, and assessing the impact of incorporating these larvae into cricket feed, we provided a sustainable solution for enhancing the efficiency of cricket farming.

2. Materials and methods

2.1. Materials

Fresh black soldier flies (*Hermetia illucens*) were sourced from a local Thai farmer-producer. To ensure the freshness and quality, they were inspected upon receipt for vitality and uniform size, and only live, active larvae were selected. The larvae were first sieved to remove residual feces and impurities, then briefly boiled (10–15 s) to kill surface bacteria - a common practice to reduce microbial load without significantly affecting the nutritional quality [35]. After boiling, the larvae were spread on a tray to dry and then stored at 4 °C until used in experiments. The initial moisture content was determined using oven drying - as outlined in ISO 1442:1973. Triplicates of approximately 5 g of biomass were dried at 105 °C for 72 h, resulting in an initial moisture content of approximately 65 ± 2 % wet basis (w.b.).

2.2. Experimental apparatus

The drying used an infrared dryer, which directed infrared radiation from the lamp onto the larvae spread on trays within the drying chamber (Fig. 1a). The control unit, see Fig. 1b, regulated the infrared lamp and blower power to maintain the desired drying temperature. The temperature controller opened the solenoid valve when the temperature dropped below the set point. Detailed preparation of the larvae is described in Section 2.1, the infrared dryer oven in Section 2.3, and the infrared drying test in Section 2.4.

In addition to the test bench described above, these instruments were used: an electronic scale (PA4102, OHAUS), a data logger (BTM-4208SD), an anemometer (UT363S), an AC monitor (D52-2066), a hot air oven (UN30, Memmert), and an infrared gas burner (538, 3.1 kW/h). The range and precision of these instruments are listed in Table 1.

2.3. Infrared dryer oven

The infrared dryer - see Fig. 1a - used was compact, with dimensions of 450 × 930 × 650 mm. The core components included a 3.1 kW infrared lamp, an electric air blower measuring 74 × 74 × 29 mm, a drying chamber equipped with trays, a K-type thermocouple, a control unit, and a heat outflow mechanism. The infrared dryer directed infrared radiation from the lamp onto the larvae spread on trays within the drying chamber. The electric air blower circulated air to ensure even heat distribution, while the K-type thermocouple monitored the temperature inside the chamber. The control unit regulated the power to the infrared lamp and the blower to maintain the desired drying temperature – see Fig. 1b. The temperature controller opened the solenoid valve when the temperature dropped below the set point. When opened, the solenoid valve released liquefied petroleum gas (LPG) through a low-pressure regulator into the infrared lamp for combustion and heat generation. Once the temperature reached the desired level, the solenoid valve closed to stop the gas flow and turn off the infrared lamp. This was continued to keep the temperature constant as the cycle repeated. To ensure consistent drying conditions, the dryer's temperature control system was calibrated and validated before use. Calibration adjusted the control unit to achieve accurate temperature settings, which were verified using the thermocouple readings at various points within the drying chamber. Validation ran a series of test drying cycles at different temperatures to confirm that the system consistently maintained the target temperatures with minimal fluctuations. This calibration and validation process was crucial to ensure that drying conditions were uniform throughout the chamber, thereby producing reliable and reproducible results.

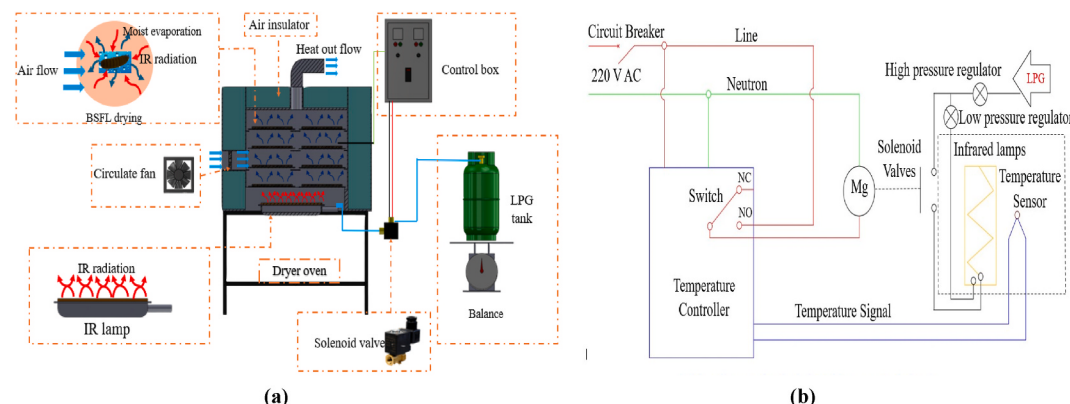


Fig. 1. (a) Infrared dryer schematic diagram, (b) Wiring diagram for control unit.

Table 1

Range and precision of the relevant experimental instrument.

Experimental instrument	Model	Range	Precision
Electronic scale	PA4102 (OHAUS)	0.1–4100 g	±0.01 g
	KA84Y/P1834 (Brifit)	0.001–200 g	±0.01 g
Data logger	BTM-4208SD	-50 – 999.9 °C	±(0.4 % + 0.5 °C)
Anemometer (wind speed)	UT363S	0.4–30 m/s	±(5 % + 0.5 m/s)
Solenoid valve	RS2554171	0–6 bar	±0.10 V
AC monitor	D52-2066	0–100.0 A	±0.01 A
Hot air oven	UN30 (Memmert)	20–300 °C	±0.10 °C
Infrared gas burner	538, 3.1 kW/h	343–1100 °C	–

2.4. Experimental infrared drying test

The infrared dryer was tested to ensure that the temperature distribution in the drying chamber was suitable for use. The drying temperatures tested were 50 °C, 60 °C, and 70 °C, with air velocities of 1.0, 1.5, and 2.0 m/s. A 100 g larvae sample was dried at the specified temperature and air speed. The mass change was recorded every 30 min until the larvae moisture content was 10 % w.b. Additionally, LPG gas consumed was recorded by weighing, and the electrical energy consumed by the blower and electric control unit was measured with an ammeter to compute the specific energy required for drying. All experimental conditions were tested in triplicate for each sample.

2.5. Black soldier fly larvae drying kinetics

Empirical mathematical models were developed and tested. The larvae moisture content obtained from the experiment in drying temperatures from 50 °C to 70 °C under air at 1.0–2.0 m/s were converted to the relative moisture ratio (MR) of larvae during drying using Equation (1) [36].

$$MR = \frac{M_t - M_{eq}}{M_0 - M_{eq}} \quad (1)$$

where M_t is the moisture content at time, t (%w.b.), M_0 is the initial moisture content (% w.b.) and M_{eq} is the equilibrium moisture content, determined from the experiment by recording the larvae mass hourly until it remained steady. Moisture ratios versus drying time were fitted to the semi-theoretical models in Table 2, which are widely used in drying kinetics [37,38]. Non-linear regressions were used to obtain the constants in each model.

The coefficient of determination, R^2 , reduced chi-squared, χ^2 , and root mean square error, RMSE, were calculated to evaluate the fit of each model to experimental data. Higher R^2 values and the lower χ^2 and RMSE values indicated better fits, following to of Midilli and Kucuk [44–50]. These metrics were calculated using Equations (2)–(4).

$$R^2 = 1 - \left(\frac{\sum_{i=1}^N (MR_{pred,i} - MR_{exp,i})^2}{\sum_{i=1}^N (MR_{pred,i} - MR_{exp,i})^2} \right) \quad (2)$$

$$\chi^2 = \frac{\sum_{i=1}^N (MR_{exp,i} - MR_{pred,i})^2}{N - n} \quad (3)$$

$$RMSE = \left(\frac{1}{N} \sum_{i=1}^N (MR_{pred,i} - MR_{exp,i})^2 \right)^{1/2} \quad (4)$$

where $MR_{exp,i}$ is the i-th experimentally observed moisture ratio, $MR_{pred,i}$ the i-th predicted moisture ratio and N is the number of

Table 2

Mathematical models for thin layer drying considered.

No.	Model	Formula	Ref
1	Newton	$MR = \exp(-kt)$	[39]
2	Page	$MR = \exp(-kt^n)$	[40]
3	Wang and Singh	$MR = 1 + at + bt^2$	[41]
4	Henderson and Pabis	$MR = a \exp(-kt)$	[42]
5	Logarithmic	$MR = a \exp(-kt) + c$	[43]
6	Midilli and Kucuk	$MR = a \exp(-kt^n) + bt$	[44]

observations and n is the number constants.

2.6. Drying indicators

2.6.1. Effective moisture diffusivity

The effective moisture diffusivity is an important material transportation property describing the drying characteristics of food. Fick's second diffusion law can be used to estimate the effective moisture diffusivity in the larvae. Crank [51] presents solutions for infinite slabs, infinite cylinders and spheres. Time integration of the analytical solution for a finite slab, gives the MR inside larvae as versus time, t , using Equation (5) [52].

$$MR = \frac{8}{\pi^2} \sum_{n=0}^{\infty} \frac{1}{(2m+1)^2} \exp \left[-\frac{(2n+1)^2 \pi^2 D_{eff} t}{4L^2} \right] \quad (5)$$

where D_{eff} is the effective water diffusion coefficient (m^2/h), L is half the material thickness (m), m is the number of experimental groups and t is the drying time (h).

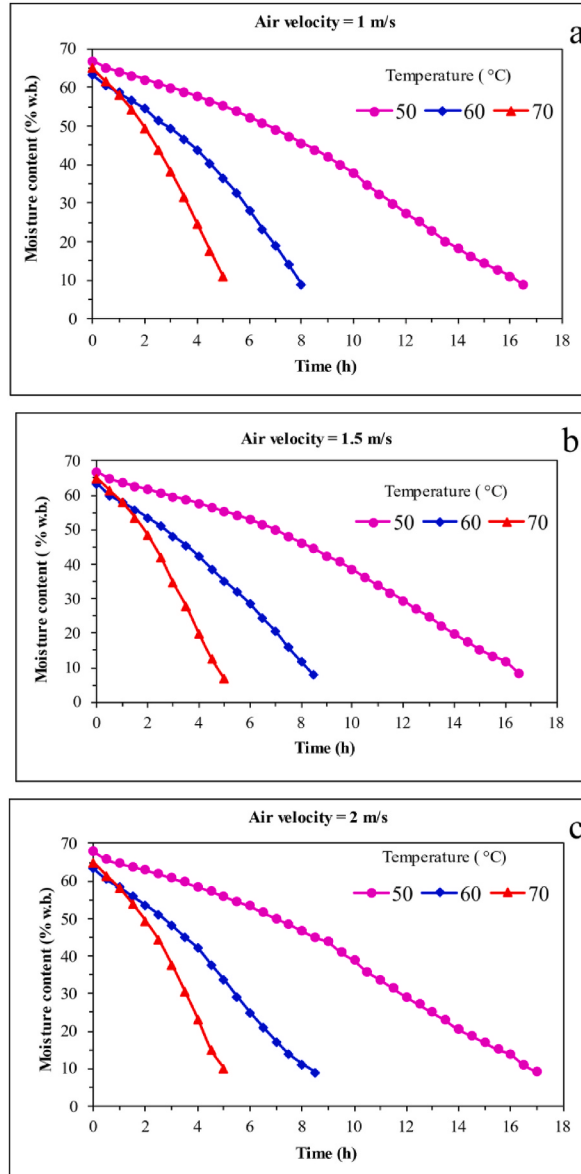


Fig. 2. Moisture content versus drying time with various temperatures and air velocities a) 1.0 m/s; b) 1.5 m/s; c) 2.0 m/s.

For long drying periods, Equation (6) can be reduced to only the first term of the series [52].

$$MR = \frac{8}{\pi^2} \exp\left(-\frac{\pi^2 D_{eff} t}{4L^2}\right) \quad (6)$$

Using the logarithmic form in Equation (7), effective moisture ratio can be calculated by plotting $\ln MR$ versus drying time, t , experimental data will give a straight line with slope, K [52]:

$$\ln MR = \ln \frac{8}{\pi^2} - \frac{\pi^2 D_{eff}}{4L^2} t \quad (7)$$

Clearly, from Equation (5), the logarithm of the moisture ratio is linearly related to the drying time: the relationship between the slope, K , and effective diffusion coefficient D_{eff} is set out in Equation (8) [44].

$$K = -\frac{\pi^2 D_{eff}}{L^2} \quad (8)$$

The temperature dependence of diffusivity was evaluated using the Arrhenius equation through nonlinear regression analysis, as shown in Equation (9) [53].

$$D_{eff} = D_0 e^{\left(\frac{-E_a}{R T}\right)} \quad (9)$$

Where E_a represents the activation energy (kJ/mol), D_0 is the pre-exponential factor (m^2/h), R is the universal gas constant (8.314 J/mol K) and T is the absolute temperature (K).

2.6.2. Energy consumption

The energy consumption of the drying equipment was measured using an ammeter (Zhejiang, China) connected to the fan and electric control unit. Additionally, the infrared lamp LPG consumption was weighed to obtain the total energy - electricity plus LPG consumption. The specific energy consumption (SEC) was calculated using Equation (10) [54].

$$SEC = \frac{Q_{total}}{W_d} \quad (10)$$

where SEC is the specific energy consumption (MJ/kg of water), Q_{total} is the total heat consumption (MJ) and W_d is the mass of water evaporated (kg).

2.7. Statistics analysis

The results for each drying condition were analyzed by ANOVA and means were compared using Tukey's Honestly Significant Difference (HSD) test with IBM SPSS Statistics Version 29.0.2.0 (IBM Corp, 2023).

3. Results and discussion

3.1. Infrared drying larvae

The drying curves illustrating the effect of temperature and air velocity on drying behaviors are shown in Fig. 2a, b, and 2c. The drying curves are characterized by a regular model, typical for colloidal-capillary-porous materials [55,56]. In this study, whole larvae were dried. This approach offers a variety of opportunities for subsequent processing or target applications. Due to their size and shape, they may be used as alternatives to textured proteins in various food products [27,57,58]. Higher temperatures led to shorter drying

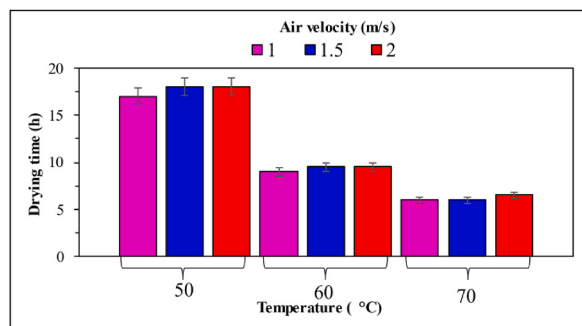


Fig. 3. Drying time versus temperatures a) 1.0 m/s; b) 1.5 m/s; c) 2.0 m/s.

times, with 70 °C taking only 5.1 h versus 8.5 h for 60 °C and 16.6 h at 50 °C. The reduction in drying time can be explained by the electroporation of the insect cell membranes, which enhanced mass transfer during drying [27]. The air velocity did not significantly affect the drying time, as shown in Fig. 3. This may be due to the larger size of the dryer in terms of width and height compared to the fan power, which caused vortices in the airflow inside the dryer before it exited. As a result, the airflow was not streamlined. However, infrared drying offered a significant advantage in reducing drying time, making it 30–50 % faster than hot air drying [29].

However, air velocity affected the larvae drying rate, calculated from the moisture over time and presented in Fig. 4a, b, and 4c. It illustrated that samples dried at different temperatures showed similar patterns. The drying rate can be classified into three regions; in the first region, initial drying rate rose to 0.25, in the second region, the drying rate changed slowly, and in the last stage, the drying rate sharply increased between 0.8 and 0.9 of MR. This last drying stage corresponds to a moisture content range of 65–54 %w.b. The higher the temperature, the higher the drying rate. Drying at 70 °C had a higher rate than temperatures of 60 °C and 50 °C as well. Due to the high temperature differential between the dried matter and the surrounding air, the moisture diffusivity to the surface was enhanced, resulting in increased water evaporation, higher mass transfer, and drying rate [27,59].

Fig. 5 presents the mean relative difference over larvae drying times at temperatures, 50 °C, 60 °C, and 70 °C, with air velocity at 1.5 m/s. The error bars represent variations of one standard deviation. Higher drying temperatures (70 °C) resulted in faster initial drying rates but exhibited higher variations (represented by larger error bars) early in drying, i.e. during the first few hours. In contrast, drying at 60 °C led to a balanced approach, achieving a relatively consistent drying rate with less variability over time compared to 50 °C. The lower temperature led to the slowest and most variable drying, particularly after 10 h, where the relative differences fluctuated significantly. However, the experimental data shows deviations of less than ±2 %.

3.2. Specific heat consumptions

Table 3 shows the energy consumption for larvae drying under different conditions of temperature and air velocity. The SEC was

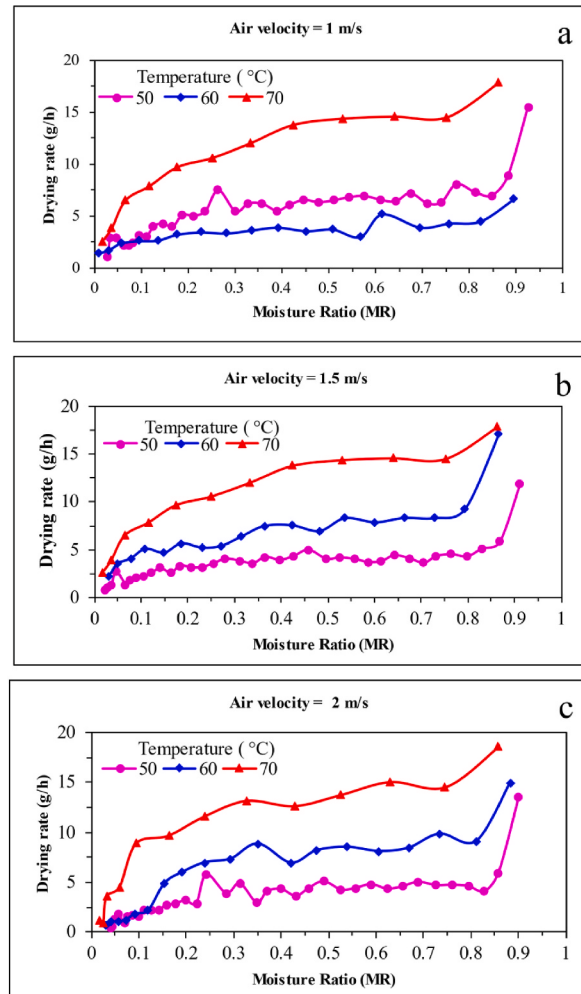


Fig. 4. Drying rate versus MR and temperature at air velocities a) 1.0 m/s; b) 1.5 m/s; c) 2.0 m/s.

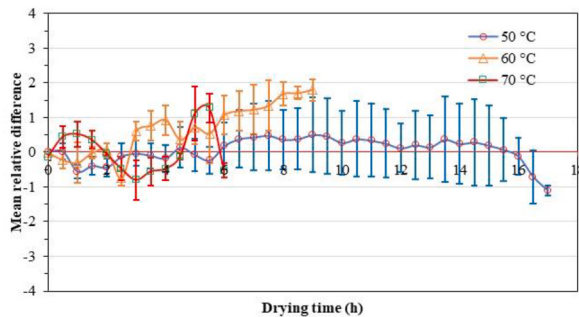


Fig. 5. Mean relative difference for the drying experiments at various temperatures with 1.5 m/s air velocity: error bars represent one standard deviation.

primarily influenced by the consumption of electricity and LPG. At a drying temperature of 60 °C, the SEC was 1.58 MJ/kg water evaporated, which was lower than the SEC at 50 °C and 70 °C. The SEC at 50 °C took a long time which led to more electricity consumption than other drying temperatures. Whereas, the LPG consumption was low because the infrared lamps were not ‘sparked’ or turned on so often.

In contrast, drying at 70 °C needed high LPG consumption (0.68–0.84 kWh), so that SEC was also high. Wang et al. [39] showed that hot air drying tended to have higher energy consumption due to the need to maintain a constant temperature throughout the drying process, often resulting in SEC values up to 2.5 MJ/kg. Additionally, solar drying led to significantly lower energy consumption, typically ranging from 0.5 to 1.0 MJ/kg, but it was less reliable [31]. Infrared drying offers a more balanced approach, providing faster drying times and moderate energy consumption, making it more efficient than hot air drying and more reliable than solar drying under controlled conditions [30].

3.3. Modeling of drying curves

The larvae drying behavior was modeled with various semi-theoretical models at air velocities from 1.0 to 2.0 m/s and temperatures from 50 °C to 70 °C. Table 4 summarizes the model constants and statistical values (R^2 , RMSE and χ^2) for air velocities of 1.0 and 2.0 m/s.

The Logarithmic (No. 5) and Midilli (No. 6) models were found to best describe the thin-layer drying characteristics of these larvae, with $R^2 > 0.99$ for all temperatures and air velocities. Fig. 6 shows that the Logarithmic and Midilli models described the drying behavior between predictions and experiment best. This was consistent with Midilli and Kucuk [44] and Akpinar et al. [45], who demonstrated the effectiveness of the Midilli model to accurately predict drying times and moisture content. However, when compared with IR drying, the solar model tended to be slightly less accurate due to the variability in drying conditions.

3.4. Effective moisture diffusivity and activation energy

Moisture diffusivities were calculated using Equation (8), representing the rate at which moisture migrates from the interior of the material to its surface, where it can evaporate into the surrounding air. The moisture diffusivity values varied in the range of 2.3×10^{-9} and $3.1 \times 10^{-8} \text{ m}^2/\text{h}$ - see Figs. 7 and 8. Note that D_{eff} increased with increasing drying temperature and changed with air velocity.

When larvae were dried at high temperatures, heat would increase the activity of internal water molecules, resulting in higher effective moisture diffusivity. Effective moisture diffusivity is influenced by various factors such as temperature, air velocity, material properties, and drying conditions. The highest D_{eff} was $3.09 \times 10^{-8} \text{ m}^2/\text{h}$ at 70 °C and an air velocity of 1.5 m/s, compared to hot air-drying values of $0.7002 \times 10^{-10} \text{ m}^2/\text{s}$ at 60 °C to $2.792 \times 10^{-10} \text{ m}^2/\text{s}$ at 90 °C [60] and 6.15×10^{-11} to $2.63 \times 10^{-10} \text{ m}^2/\text{s}$ for

Table 3
Specific energy consumption.

Condition	Temp. (°C)	Air velocity (m/s)	Drying time (h)	Energy (kWh)				SEC (MJ/kg)
				Blower	Controller	LPG	Total	
50	1		17.5	0.168	0.630	0.195	0.993	1.819
	1.5		18	0.172	0.648	0.190	1.01	1.850
	2		18	0.172	0.648	0.190	1.01	1.850
60	1		9	0.086	0.342	0.456	0.866	1.584
	1.5		9.5	0.091	0.342	0.432	0.865	1.584
	2		9.5	0.091	0.342	0.432	0.865	1.584
70	1		6	0.057	0.216	0.684	0.958	1.754
	1.5		6	0.057	0.216	0.684	0.958	1.754
	2		6.5	0.062	0.234	0.842	1.139	2.085

Table 4

Model constants and statistic values of each mathematical model at an air velocity of 1.0 and 2.0 m/s.

Model	Temp. (°C)	Model constants	R ²	RMSE	χ^2
Air velocity 1.0 m/s					
1	50	k = 0.123	0.9648	0.0001	0.0004
	60	k = 0.233	0.9577	6.89×10^{-5}	0.0001
	70	k = 0.386	0.966	5.03×10^{-5}	0.0001
2	50	k = 0.064, n = 1.332	0.9899	0.0014	0.003
	60	k = 0.131, n = 1.376	0.9869	0.0009	0.0021
	70	k = 0.253, n = 1.395	0.9947	0.005	0.0118
3	50	a = -0.089, b = 0.002	0.9984	0.005	0.0106
	60	a = -0.163, b = 0.006	0.9989	0.0008	0.0019
	70	a = -0.278, b = 0.019	0.9992	0.3418	0.8079
4	50	k = 0.131, a = 1.062	0.9701	0.0017	0.0035
	60	k = 0.249, a = 1.064	0.964	0.0009	0.0021
	70	k = 0.412, a = 1.068	0.9728	0.0008	0.0019
5	50	k = 0.060, a = 1.526, c = -0.537	0.9981	3.70×10^{-5}	8.08×10^{-5}
	60	k = 0.094, a = 1.758, c = -0.768	0.9989	1.92×10^{-5}	4.55×10^{-5}
	70	k = 0.221, a = 1.399, c = -0.384	0.9977	5.29×10^{-7}	1.38×10^{-6}
6	50	k = 0.058, n = 1.205, a = 0.962, b = -0.008	0.9981	0.0002	0.0004
	60	k = 0.133, n = 1.024, a = 0.989, b = -0.032	0.9989	5.77×10^{-5}	0.0001
	70	k = 0.246, n = 1.247, a = 0.989, b = -0.017	0.9992	2.49×10^{-7}	7.18×10^{-7}
Air velocity 2.0 m/s					
1	50	k = 0.127	0.9733	0.0005	0.0011
	60	k = 0.249	0.973	9.21×10^{-5}	0.0002
	70	k = 0.397	0.9665	0.0002	0.0003
2	50	k = 0.073, n = 1.258	0.9898	0.0013	0.0028
	60	k = 0.158, n = 1.302	0.9934	0.0004	0.001
	70	k = 0.257, n = 1.403	0.9945	0.0067	0.0157
3	50	a = -0.095104, b = 0.002	0.9967	0.0146	0.0308
	60	a = -0.184, b = 0.009	0.9998	0.0023	0.0051
	70	a = -0.288, b = 0.214	0.9975	0.8171	1.9066
4	50	k = 0.133, a = 1.042	0.9756	0.0013	0.0027
	60	k = 0.263, a = 1.056	0.9774	0.0008	0.0018
	70	k = 0.423, a = 1.072	0.9726	0.0012	0.0027
5	50	k = 0.073, a = 1.334, c = -0.354	0.9964	1.10×10^{-5}	2.40×10^{-5}
	60	k = 0.154, a = 1.304, c = -0.302	0.9967	2.38×10^{-6}	5.59×10^{-6}
	70	k = 0.258, a = 1.290, c = -0.269	0.9945	1.85×10^{-8}	4.71×10^{-8}
6	50	k = 0.060, n = 1.243, a = 0.944, b = -0.005	0.9970	2.49×10^{-5}	5.59×10^{-5}
	60	k = 0.152, n = 1.212, a = 0.973, b = -0.009	0.9978	3.78×10^{-6}	9.45×10^{-6}
	70	k = 0.244, n = 1.333, a = 0.979, b = -0.009	0.9973	1.53×10^{-5}	4.28×10^{-5}

temperatures ranging from 40 °C to 70 °C [53]. Higher temperatures generally increased diffusivity by providing more energy for moisture transfer, while higher air velocities enhanced convective heat and mass transfer, thereby increasing diffusivity as well [51]. Infrared drying enhances moisture diffusivity through direct heat application, which accelerated drying and improved overall efficiency compared with hot air drying and solar drying [45].

Fig. 9 presents the E_a calculated by plotting $\ln(D_{eff})$ against the reciprocal of temperature (1/T), showing a linear relationship where the slope represents $-Ea/R$. The resulting activation energy values range from 56.88 kJ/mol at 1.0 m/s air velocity to 115.41 kJ/mol at 2.0 m/s air velocity. These values are similar to activation energies reported for BSFL drying using hot air: 48.66 kJ/mol [53] and 43.97 kJ/mol [60]. Additionally, these values fall within the broader range typically observed in food materials, which is between 12.7 and 110 kJ/mol [61].

4. Conclusion

This study demonstrated the efficacy of infrared drying as an innovative method for processing Black Soldier Fly Larvae (BSFL) into high-quality feed ingredients for cricket farming. Infrared drying at 70 °C achieved optimal drying times of 5.1 h, with the least energy-efficient performance at 60 °C (1.58 MJ/kg water evaporated). The logarithmic and Midilli models accurately described the drying kinetics ($R^2 > 0.99$), while effective moisture diffusivity ranged from 2.28×10^{-9} to $3.09 \times 10^{-8} \text{ m}^2/\text{h}$, peaking at 70 °C and 1.5 m/s air velocity. Activation energy values spanned from 56.88 kJ/mol at 1.0 m/s to 115.41 kJ/mol at 2.0 m/s air velocity. Although this study does not include direct comparisons with conventional methods like hot-air or freeze drying, existing literature indicates that these methods generally require longer drying times and consume more energy. Future research should focus on direct comparisons between infrared drying and these traditional methods to quantify their relative efficiencies. Additionally, further studies should examine the scalability of infrared drying, assess the nutritional quality and palatability of dried BSFL in cricket diets, conduct economic analyses, and explore applications for other insect species. This study provides a foundation for integrating infrared-dried BSFL into cricket feed, offering a promising pathway towards more sustainable and efficient insect farming practices in the face of growing global demand for

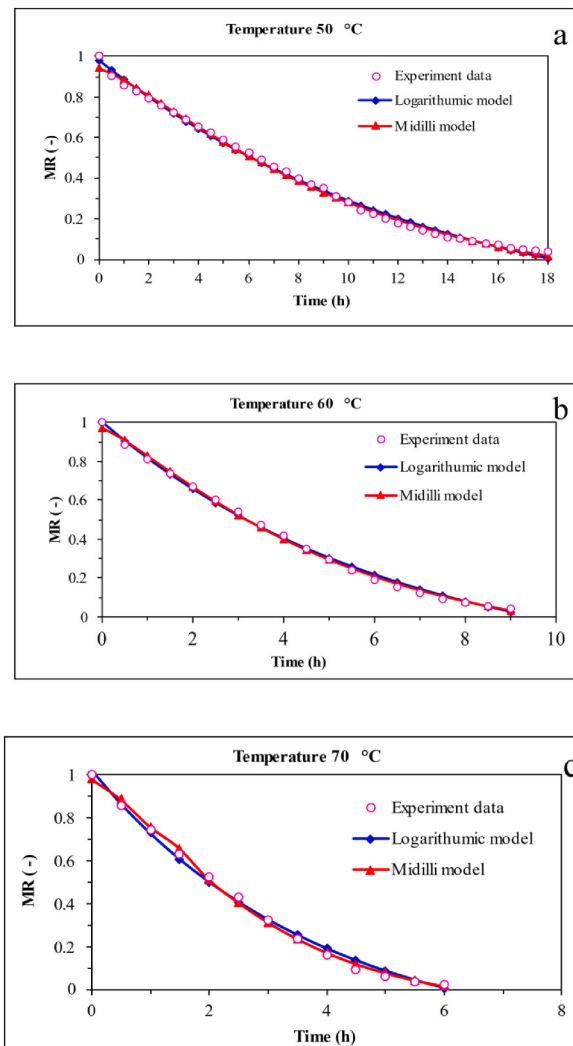


Fig. 6. MR versus drying time at air velocity 2.0 m/s for experimental data and logarithmic and Midilli models at a) 50 °C, b) 60 °C, and c) 70 °C.

alternative protein sources. Future studies will focus on examining the nutritional quality attributes, such as protein retention and lipid oxidation, to further support the suitability of infrared-dried BSFL in feed production.

CRediT authorship contribution statement

Nuntawat Butwong: Writing – original draft, Methodology, Investigation. **Sarawut Saenkhamp:** Methodology, Investigation, Data curation. **Adisak Pattiya:** Writing – review & editing. **Anuwat Saenpong:** Resources. **Chinnapat Turakarn:** Resources. **Aphichon Mungchu:** Resources. **Shenghua Hu:** Data curation. **Sopa Cansee:** Writing – review & editing, Funding acquisition, Conceptualization.

Declaration of generative AI in scientific writing

During the preparation of this work, we used Chat GPT 4o in order to cover of review related paper research. After using this tool, we reviewed and edited the content as needed and take responsibility for the content of this article.

Declaration of competing interest

The authors declare the following financial interests/personal relationships which may be considered as potential competing interests: Sopa Cansee reports financial support was provided by Mahasarakham University, Thailand. Sopa Cansee reports a relationship with Mahasarakham University that includes: employment. If there are other authors, they declare that they have no known competing

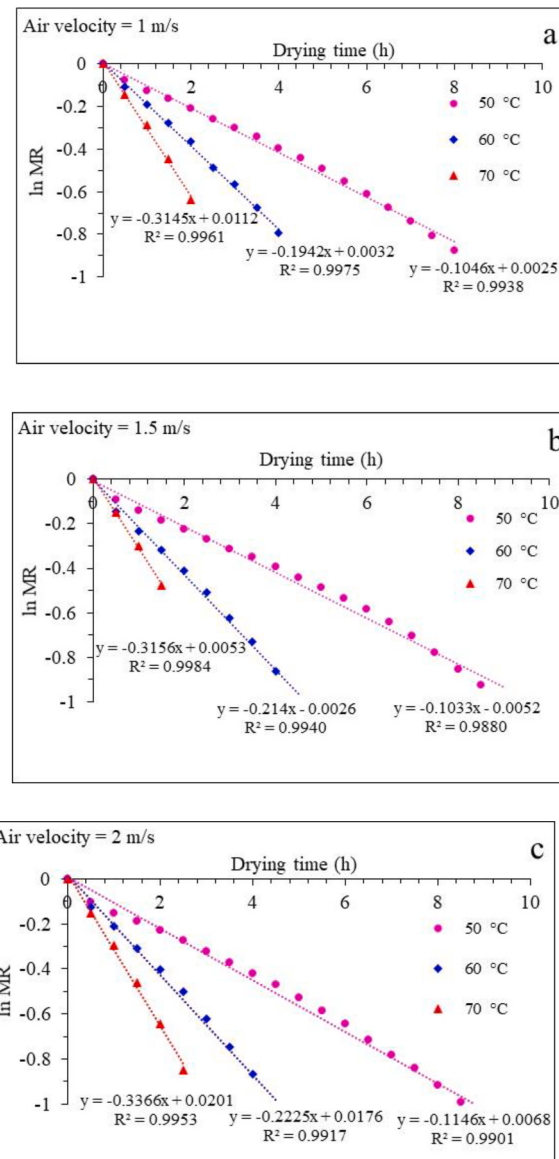


Fig. 7. ln (MR) versus drying time at air velocities of a) 1.0, b) 1.5, and c) 2.0 m/s.

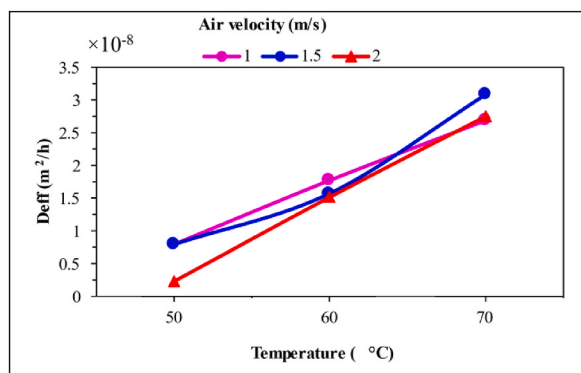


Fig. 8. D_{eff} versus drying temperature at different air velocities.

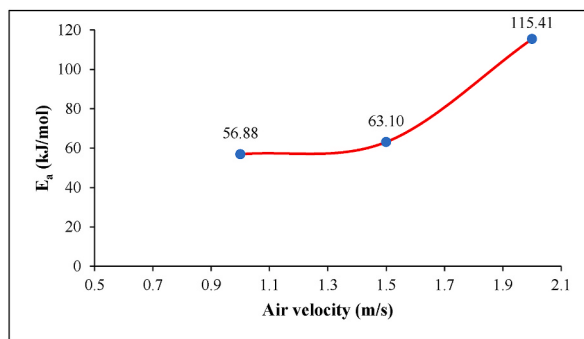


Fig. 9. E_a versus air velocity at drying temperatures ranging from 50 °C to 70 °C.

financial interests or personal relationships that could have appeared to influence the work reported in this paper.

Acknowledgement

This research project was financially supported by Mahasarakham University.

Nomenclature

<i>a</i>	Dimensionless drying constant
<i>b</i>	Dimensionless drying constant
<i>c</i>	Dimensionless drying constant
<i>n</i>	Dimensionless drying constant
<i>k</i>	Drying velocity constant (1/h)
MR	Moisture ratio
M_t	Moisture content at t (%w.b.)
M_0	Initial moisture content (%w.b.)
M_{eq}	Moisture content in equilibrium (%w.b.)
R^2	Coefficient of determination
χ^2	Chi-square
RMSE	Root mean square error
$MR_{exp,i}$	Experimental moisture ratio
$MR_{pre,i}$	Predicted moisture ratio
N	Number of observations
n	Number of constants
D_{eff}	Effective water diffusion coefficient (m^2/h)
L	Half the material thickness (m)
<i>m</i>	Number of experimental groups
<i>t</i>	Drying time (h)
<i>K</i>	Slope
E_a	Activation energy (kJ/mol)
D_0	Pre-exponential factor (m^2/h)
R	Universal gas constant (8.314 J/mol K)
T	Absolute temperature (K)
SEC	Specific energy consumption (MJ/kg of water)
Q_{total}	Total heat consumption (MJ)
W_d	Mass of water evaporated (kg)
Abbreviation	
ANOVA	Analysis of variance
BSFL	Black soldier fly larvae
FIR	Far-infrared radiation
HSD	Tukey's honestly significant difference test
IR	Infrared ray
LPG	Liquefied petroleum gas
NIR	Near-infrared

Data availability

Data will be made available on request.

References

- [1] Food and Agriculture Organization of the United Nations, How to feed the world, High-level expert forum, Food and Agriculture Organization of the United Nations (2024) [Retrieved August 24, 2024], from, <https://www.fao.org/wfs/forum>.
- [2] A. Van Huis, Potential of insects as food and feed in assuring food security, *Annu. Rev. Entomol.* 58 (1) (2013) 563–583.
- [3] W.H. Organization, The state of food security and nutrition in the world, Building climate resilience for food security and nutrition, Food and Agriculture Organization of the United Nations (2018) [Retrieved August 24, 2024], from, <http://www.fao.org/3/19553EN/19553en.pdf>.
- [4] G. Bosch, S. Zhang, D.G. Oonincx, W.H. Hendriks, Protein quality of insects as potential ingredients for dog and cat foods, *J. Nutr. Sci.* 3 (2014) e29.
- [5] A. Van Huis, Insects as food and feed, a new emerging agricultural sector: a review, *J. Insects Food Feed.* 6 (1) (2020) 27–44.
- [6] G.R. DeFoliart, Insects as food: why the western attitude is important, *Annu. Rev. Entomol.* 44 (1) (1999) 21–50.
- [7] T. Veldkamp, et al., Insects as a sustainable feed ingredient in pig and poultry diets: a feasibility study, *Wageningen UR Livest. Res* (2012) 1570–8616.
- [8] M.J. Sanchez-Muros, F.G. Barroso, F. Manzano-Agugliaro, Insect meal as renewable source of food for animal feeding: a review, *J. Clean. Prod.* 65 (2014) 16–27.
- [9] D.C. Sheppard, G.L. Newton, S.A. Thompson, S. Savage, A value added manure management system using the black soldier fly, *Bioresour. Technol.* 50 (3) (1994) 275–279.
- [10] J.K. Tomberlin, D.C. Sheppard, J.A. Joyce, Black soldier fly larvae: a promising resource for organic waste conversion and recovery, *Waste Manag. Res.* 20 (2) (2002) 100–108.
- [11] W.T. Kim, et al., Characterization of the molecular features and expression patterns of two serine proteases in *Hermetia illucens* (Diptera: stratiomyidae) larvae, *BMB Rep* 44 (6) (2011) 387–392.
- [12] H. Cickova, G.L. Newton, R.C. Lacy, M. Kozanek, The use of fly larvae for organic waste treatment, *Waste Manag.* 35 (2015) 68–80.
- [13] S. Diener, et al., Black soldier fly larvae for organic waste treatment-prospects and constraints, *Proc. WasteSafe.* (2011) 13–15.
- [14] T.R. Green, R. Popa, Enhanced ammonia content in compost leachate processed by black soldier fly larvae, *Appl. Biochem. Biotechnol.* 166 (2012) 1381–1387.
- [15] G.R. Gujarathi, M.K. Pejaver, Occurrence of Black Soldier Fly *Hermetia illucens* (Diptera: Stratiomyidae) in Biocompost, 2013.
- [16] M. Kalova, M. Borkovcova, Voracious larvae *Hermetia illucens* and treatment of selected types of biodegradable waste, *Acta Univ. Agric. Silvic. Mendelianae Brnoensis* 61 (1) (2013) 77–83.
- [17] R. Rachmawati, D. Buchori, P. Hidayat, S. Hem, M.R. Fahmi, Perkembangan dan kandungan nutrisi larva *Hermetia illucens* (Diptera: stratiomyidae) pada bungkil kelapa sawit, *J. Entomol. Indones.* 7 (1) (2010), 28–28.
- [18] K.B. Barragan-Fonseca, J. Pineda-Mejia, M. Dicke, J.J. van Loon, Insects for sustainable animal feed: the case of black soldier fly, *J. Insects Food Feed.* 3 (2) (2017) 117–130.
- [19] H.M. Myers, J.K. Tomberlin, B.D. Lambert, D. Kattes, Development of black soldier fly (Diptera: stratiomyidae) larvae fed dairy manure, *Environ. Entomol.* 37 (1) (2014) 11–15.
- [20] T.T. Nguyen, J.K. Tomberlin, S. Vanlaerhoven, Influence of resources on *Hermetia illucens* (Diptera: stratiomyidae) larval development, *J. Med. Entomol.* 50 (4) (2013) 898–906.
- [21] L. Newton, C. Sheppard, D.W. Watson, G. Burtle, R. Dove, Using the black soldier fly, *Hermetia illucens*, as a value-added tool for the management of swine manure, Animal and Poultry Waste Management Center, North Carolina State University 17 (18) (2005). Raleigh, NC.
- [22] S. Diener, C. Zurbrugg, K. Tockner, Conversion of organic material by black soldier fly larvae: establishing optimal feeding rates, *Waste Manag. Res.* 27 (6) (2009) 603–610.
- [23] C. Lalander, S. Diener, M.E. Magri, C. Zurbrugg, A. Lindstrom, B. Vinneras, Faecal sludge management with the larvae of the black soldier fly (*Hermetia illucens*)-From a hygiene aspect, *Sci. Total Environ.* 458 (2013) 312–318.
- [24] D.G. Oonincx, S. Van Broekhoven, A. Van Huis, J.J. Van Loon, Feed conversion, survival and development, and composition of four insect species on diets composed of food by-products, *PLoS One* 10 (12) (2015) e0144601.
- [25] M. Henry, L. Gasco, G. Piccolo, E. Fountoulaki, Review on the use of insects in the diet of farmed fish: past and future, *Anim. Feed Sci. Technol.* 203 (2015) 1–22.
- [26] J. Larouche, Processing Methods for the Black Soldier Fly (*Hermetia illucens*) Larvae: from Feed Withdrawal Periods to Killing Methods, 2019.
- [27] R. Bogusz, et al., The selected quality aspects of infrared-dried black soldier fly (*Hermetia illucens*) and yellow mealworm (*Tenebrio molitor*) larvae pre-treated by pulsed electric field, *Innovat. Food Sci. Emerg. Technol.* 80 (2022) 103085.
- [28] D.A. Tzompá-Sosa, L. Yi, H.J. van Valenberg, M.A. van Boekel, C.M. Lakemond, Insect lipid profile: aqueous versus organic solvent-based extraction methods, *Food Res. Int.* 62 (2014) 1087–1094.
- [29] D. Nowak, P.P. Lewicki, Infrared drying of apple slices, *Innovat. Food Sci. Emerg. Technol.* 5 (3) (2004) 353–360.
- [30] K. Krishnamurthy, H.K. Khurana, J. Soojin, J. Irudayaraj, A. Demirci, Infrared heating in food processing: an overview, *Compr. Rev. Food Sci. Food Saf.* 7 (1) (2008) 2–13.
- [31] K. Chua, S. Chou, Low-cost drying methods for developing countries, *Trends Food Sci. Technol.* 14 (12) (2003) 519–528.
- [32] Y. Sui, J. Yang, Q. Ye, H. Li, H. Wang, Infrared, convective, and sequential infrared and convective drying of wine grape pomace, *Dry. Technol.* 32 (6) (2014) 686–694.
- [33] S. Mongpraneet, T. Abe, T. Tsurusaki, Accelerated drying of Welsh onion by far infrared radiation under vacuum conditions, *J. Food Eng.* 55 (2) (2002) 147–156.
- [34] S. Devahastin, Drying of Foods and Biomaterials, Bangkok, TopPublisher, 2012.
- [35] E. Nyakeri, H. Ogola, M. Ayieko, F. Amimo, An open system for farming black soldier fly larvae as a source of proteins for smallscale poultry and fish production, *J. Insects Food Feed.* 3 (1) (2017) 51–56.
- [36] A. Lammerskitten, et al., Impact of pulsed electric fields on physical properties of freeze-dried apple tissue, *Innovat. Food Sci. Emerg. Technol.* 57 (2019) 102211.
- [37] E.K. Akpinar, Mathematical modelling and experimental investigation on sun and solar drying of white mulberry, *J. Mech. Sci. Technol.* 22 (2008) 1544–1553.
- [38] M. Peter, et al., Computational intelligence and mathematical modelling in chanterelle mushrooms' drying process under heat pump dryer, *Biosyst. Eng.* 212 (2021) 143–159.
- [39] H. Wang, M. Zhang, A.S. Mujumdar, Comparison of three new drying methods for drying characteristics quality of shiitake mushroom (*Lentinus edodes*), *Dry. Technol.* 32 (15) (2014) 1791–1802.
- [40] K. Sacilik, R. Keskin, A.K. Elicin, Mathematical modelling of solar tunnel drying of thin layer organic tomato, *J. Food Eng.* 73 (3) (2006) 231–238.
- [41] G.Y. Wang, R. Singh, Single Layer Drying Equation for Rough Rice, 1978. ASAE Paper No. 3001.
- [42] G.E. Page, Factors Influencing the Maximum Rates of Air Drying Shelled Corn in Thin Layers, Purdue University, Lafayette, 1949.
- [43] L.R. Verma, R.A. Bucklin, J.B. Endan, F.T. Wratten, Effects of drying air parameters on rice drying models, *Trans. ASAE Am. Soc. Agric. Eng.* 28 (1) (1985) 296–301.
- [44] A. Midilli, H. Kucuk, Mathematical modeling of thin layer drying of pistachio by using solar energy, *Energy Convers. Manag.* 44 (7) (2003) 1111–1122.
- [45] E.K. Akpinar, Y. Bicer, F. Cetinkaya, Modelling of thin layer drying of parsley leaves in a convective dryer and under open sun, *J. Food Eng.* 75 (3) (2006) 308–315.
- [46] W. Asiru, A. Raji, J. Igbeke, G. Elemo, Mathematical modelling of thin layer dried cashew kernels, *Niger. Food J.* 31 (2) (2013) 106–112.
- [47] W.P. Da Silva, C.M. e Silva, F.J. Gama, J.P. Gomes, Mathematical models to describe thin-layer drying and to determine drying rate of whole bananas, *J. Saudi Soc. Agric. Sci.* 13 (1) (2014) 67–74.
- [48] A.O. Omolade, P.F. Kapila, H.M. Silungwe, Mathematical modeling of drying characteristics of Jew's mallow (*Corchorus olitorius*) leaves, *Inf. Process. Agric.* 6 (1) (2019) 109–115.
- [49] O. Alara, N. Abdurahman, O. Olalere, Mathematical modelling and morphological properties of thin layer oven drying of *Vernonia amygdalina* leaves, *J. Saudi Soc. Agric. Sci.* 18 (3) (2019) 309–315.

- [50] T.N.T. Tran, et al., Modelling drying kinetic of oyster mushroom dehydration—The optimization of drying conditions for dehydratation of Pleurotus species, *Mater. Sci. Energy Technol.* 3 (2020) 840–845.
- [51] J. Crank, *The Mathematics of Diffusion*, Oxford University Press, 1979.
- [52] Y. Du, J. Yan, H. Wei, H. Xie, Y. Wu, J. Zhou, Drying kinetics of paddy drying with graphene far-infrared drying equipment at different IR temperatures, radiations-distances, grain-flow, and dehumidifying-velocities, *Case Stud. Therm. Eng.* 43 (2023) 102780.
- [53] M. Lehmad, Y. El Hachimi, P. Lhomme, S. Mgħazli, N. Abdenouri, Comprehensive analysis of adsorption–desorption isotherms, drying kinetics, and nutritional quality of Black Soldier Fly (*Hermetia illucens*) larvae, *Food Biophys.* 19 (4) (2024) 938–954.
- [54] Y. Abbaspour-Gilandeh, M. Kaveh, H. Fatemi, E. Khalife, D. Witrowa-Rajchert, M. Nowacka, Effect of pretreatments on convective and infrared drying kinetics, energy consumption and quality of terebinth, *Appl. Sci.* 11 (16) (2021) 7672.
- [55] R. Polak, A. Krzykowski, S. Rudy, B. Biernacka, D. Dziki, Analiza Kinetyki Sublimacyjnego Suszenia Lisci Lubczyku Ogrodowego (Levisticum Officinale Koch.), *Zesz. Probl. Postępow Nauk Roln.* 2017, p. 591.
- [56] A. Krzykowski, S. Rudy, R. Polak, D. Dziki, B. Biernacka, R. Rozyło, Analiza Procesu Konwekcyjno-Mikrofalowego Suszenia Plastrow Cebuli, MOTROL, 2017, p. 55.
- [57] T.K. Kim, H.I. Yong, J.Y. Cha, S.Y. Park, S. Jung, Y.S. Choi, Drying-induced restructured jerky analog developed using a combination of edible insect protein and textured vegetable protein, *Food Chem.* 373 (2022) 131519.
- [58] M. Mishyna, J. Chen, O. Benjamin, Sensory attributes of edible insects and insect-based foods—Future outlooks for enhancing consumer appeal, *Trends Food Sci. Technol.* 95 (2020) 141–148.
- [59] M. Kaveh, Y. Abbaspour-Gilandeh, E. Taghinezhad, D. Witrowa-Rajchert, M. Nowacka, The quality of infrared rotary dried terebinth (*Pistacia atlantica* L.)—optimization and prediction approach using response surface methodology, *Molecules* 26 (7) (2021) 1999.
- [60] M.C. Pinheiro, N. Ribeiro, P. da Silva, R. Costa, Black soldier fly, *L. Hermetia illucens*, Larvae for food and feed: modelling drying kinetics, *J. Insects Food Feed* 8 (5) (2022) 469–480.
- [61] N.P. Zogzas, Z.B. Maroulis, D. Marinos-Kouris, Moisture diffusivity data compilation in foodstuffs, *Dry. Technol.* 14 (10) (1996) 2225–2253.